Propagation and Radiation Characteristics of a Multimode Corrugated Waveguide Feedhorn

D. Hoppe
Radio Frequency and Microwave Subsystems Section

This report describes a prototype of the multimode corrugated feedhorn which will be used in the 400 kW CW Ka-band radar system. A rough design is done using coupled mode theory and standard corrugated waveguide modes. A more exact analysis using mode matching techniques is then used which takes into account the effect of a finite number of corrugations per wavelength and determines the modes which are reflected from the device. A prototype feedhorn has been constructed and measured. These experimental results are then compared to the theoretical predictions which agree satisfactorily closely.

I. Introduction

A previous report described a conceptual design for a 400 kW CW Ka-band radar transmitter (Ref. 1). In order to transport this large amount of CW millimeter wave power, a multimode transmission line must be used. By using optimally designed waveguide tapers, mode converters, and monitoring devices nearly all of the microwave power at the end of the transmission line will be contained in a rotating TE_{11} circular waveguide mode. The chosen diameter of the multimode waveguide system is essentially the correct size for optimally illuminating the subreflector, but the beamwidth in the E and H planes should be equalized for best antenna efficiency (Ref. 2). Equal E and H plane beamwidths may be obtained by transforming the TE_{11} mode into the balanced HE_{11} mode in multimode corrugated waveguide. This report describes the theoretical and experimental results for a multimode corrugated waveguide section that accomplishes the above transformation.

II. Theory

Two types of horn antenna possessing equal E and H plane patterns are commonly used. The first is the dual mode horn (Ref. 3), and the second is the corrugated horn (Ref. 4).

In the dual mode horn a dominant mode circular waveguide is connected to another guide of slightly larger diameter, where modes up to TM_{11} may propagate, via a step transition.

The step size is chosen to generate the precise amount of TM_{11} mode from the TE_{11} mode so that when the two modes travel through the flared horn section which follows, the E and H plane patterns are equalized. The bandwidth of this horn is limited since the two modes must arrive at the horn aperture in phase, and the two modes have phases velocities which vary differently with frequency.

In the corrugated horn the single mode smooth wall waveguide is connected to a corrugated waveguide which supports only the HE_{11} mode. Some matching between the waveguides is provided by gradually changing from $\lambda/2$ slot depth to $\lambda/4$ slot depth in a short transition region. Throughout the transition region only the HE_{11} corrugated waveguide mode may propagate, and the E and H plane radiation patterns of this mode become nearly equal when the balanced condition is reached (slot depth $\approx \lambda/4$). The bandwidth of this horn is larger than that of the dual mode horn since the transverse electric field pattern and hence the radiation pattern of the HE_{11} mode are relatively insensitive to small changes in slot depth around the balanced condition (slot depth $\approx \lambda/4$). After the HE_{11} mode is established in the single mode corrugated waveguide, the guide is gradually flared, without changing the slot depth, to the required aperture size.

Special problems arise when multimode smooth and corrugated waveguides are used. In the specific system considered in Ref. 1 a 1.75″ I.D. circular waveguide is used at 34.0 GHz allowing over 100 waveguide modes to propagate. The radiation pattern of the TE_{11} mode from the open ended multimode waveguide may be improved by either abruptly converting some of the energy to the TM_{11} mode, as in the dual mode horn, or gradually changing the TE_{11} mode into the balanced HE_{11} mode as in the corrugated horn.

Any attempts to mimic the performance of the step in the dual mode horn in a multimode waveguide are unsuccessful, since a single step transition, slot, or iris generates a large number of modes other than TM_{11}. These modes ruin the pattern symmetry of the TE_{11} - TM_{11} combination.

The second alternative is to gradually change the TE_{11} mode into the HE_{11} mode using a multimode corrugated waveguide in which the slot depths change from $\approx \lambda/2$ to $\approx \lambda/4$. A cut-away view of such a device is shown in Fig. 1. Under multimode conditions new problems arise in making this transition. A 1.75″ diameter corrugated waveguide operated at 34.0 GHz also supports many propagating modes, even when the slot depth is constant. When the depth is changed along the guide, coupling occurs between the various corrugated waveguide modes (Ref. 5), in much the same way as radius changes in smooth multimode waveguide cause mode conversion.

The smooth walled circular waveguide may be considered to be a special case of corrugated waveguide for which the slot depth is zero or $\lambda/2$ at the operating frequency. The propagation in a corrugated waveguide of varying or constant slot depth, D, may be written in terms of coupled wave equations (Ref. 6):

$$\frac{d}{dz} A_i(z) = -j\beta_i(D) A_i(z) - \sum_{\substack{j=1 \\ j \neq i}}^{N} C_{ij}(D) \frac{dD}{dz} A_j(z) \quad i = 1, \ldots, N \tag{1}$$

In this equation $A_i(z)$ is the amplitude of the ith corrugated waveguide mode and $\beta_i(D)$ is the phase constant of the ith mode, which is a function of the slot depth at the particular value of z. If the slot depth is changing along the guide ($dD/dz \neq 0$), then coupling occurs between the possible corrugated waveguide modes. The magnitude of the coupling between modes i and j is represented by $C_{ij}(D)$, and it varies approximately as $1/[\beta_i(D) - \beta_j(D)]$, becoming larger for modes with more equal phase velocities. The quantity $\beta(D)$ is found by solving a transcendental equation whose solutions depend on the guide slot depth. For slot depth = 0 or $\lambda/2$, the solutions reduce to those corresponding to TE and TM modes in the smooth walled waveguide. For depths of approximately $\lambda/4$ and $3\lambda/4$ the solutions are those corresponding to the balanced HE and EH modes of corrugated waveguide. The root for the TE_{11} mode (1.841), $D = \lambda/2$, changes to that of the balanced HE_{11} mode ($\approx$2.401) as D decreases to $\lambda/4$. If the coupling term in Eq. (1) is neglected, then we find that the TE_{11} to balanced HE_{11} mode conversion is perfect (100%). This is the case when only one mode propagates in the guide, as in the transition section of the standard corrugated horn.

In the case of a multimode corrugated waveguide where D changes from $\lambda/2$ to $\lambda/4$, the TE_{11} - HE_{11} branch is only coupled significantly to the TM_{11} to EH_{12} branch, which has the closest phase constant. In this case Eq. (1) may be rewritten:

$$\begin{aligned} \frac{d}{dz} A_1(z) &= -j\beta_1(D) A_1(z) - C_{12}(D) \frac{dD}{dz} A_2(z) \\ \frac{d}{dz} A_2(z) &= -j\beta_2(D) A_2(z) - C_{21}(D) \frac{dD}{dz} A_1(z) \end{aligned} \tag{2}$$

Here,

$A_1(0)$ = TE_{11} input power

$A_2(0)$ = TM_{11} input power = 0

$A_1(\ell)$ = HE_{11} output power

$A_2(\ell)$ = EH_{12} output power

ℓ = transition section length

The design objective is to determine a slot depth profile where D varies from $\lambda/2$ to approximately $\lambda/4$ which maximizes $A_1(\ell)$, and minimizes $A_2(\ell)$ when Eqs. (2) are solved numerically. Several profiles for the slot depth variation were considered, including a linear profile, and one which provides constant coupling along the transition section, making

$$C_{12}(D)\,\frac{dD}{dz} = K \tag{3}$$

where K is a constant (Ref. 6). Of the profiles examined, this profile gave maximum conversion efficiency in a minimum length ℓ. For this profile the slot depth changes most gradually near depths of $\lambda/2$, where the phase constants of the two branches are closest, and more rapidly as D approaches $\lambda/4$. This profile was chosen for the actual device which was built and tested.

Certain assumptions are made in the above analysis. In particular, an ideal corrugated waveguide is modeled where an infinite number of slots per wavelength are assumed. Reflections are ignored, and only the main coupling interaction is considered. A more exact analysis of the problem which eliminates all of these faults can be undertaken. In this method the corrugated waveguide is modeled as a large number of straight waveguide sections of different radii which are connected in series. Electric fields are described as sums of smooth walled circular waveguide modes, and are matched at each of the discontinuities. The result is a scattering matrix which relates the reflected circular waveguide modes at the input to the device and the output modes, to the incident modes at the input end. The theory of this approach is given in detail by James (Ref. 7), and a computer code to carry out the computations has been written by the author[1] (see also Ref. 8, section B). The scattering matrix approach may be summarized by two matrix equations:

$$\begin{aligned} \boldsymbol{b}_1 &= [S_{11}]\,\boldsymbol{a}_1 \\ \boldsymbol{b}_2 &= [S_{21}]\,\boldsymbol{a}_1 \end{aligned} \tag{4}$$

Here $\boldsymbol{a}_1$ contains the input mode amplitudes, $\boldsymbol{b}_1$ the reflected modes, and $\boldsymbol{b}_2$ the output modes. The matrices $[S_{11}]$ and $[S_{21}]$ are scattering matrices which are determined by the computer code. Their entries are a function of frequency and device geometry. This computer program was used extensively in another development (Ref. 8), which calculated the theoretical radiation patterns for the feed under different excitation conditions.

A device of the type described above was designed using the simple coupled mode theory. The more exact scattering matrix theory was then used to predict the radiation patterns and reflection characteristics of the corrugated waveguide section. The part was then built and measured on the antenna range. These theoretical and experimental results are described in the next section.

III. Calculated and Experimental Results

The experimental model of the corrugated feed consisted of 92 slots cut in the wall of a 1.75 inch I.D. circular waveguide. The width of the slots and lands was chosen to be 0.035 inch. These parameters were chosen for the test device for several reasons. First, Eq. (2) was solved for a device of various lengths using the constant coupling slot depth profile. From this rough analysis it was found that feed lengths in excess of 15λ gave an HE_{11} mode purity level above 95%. Next a very conservative number of slots per wavelength, 5, was chosen for the test device. The final consideration was the machining complexity. It was decided to keep the number of slots under 100, and 92 were chosen which corresponded to an HE_{11} mode purity of 96.5% from the simple analysis. The slot depth profile was determined by the methods described in the previous section, and each slot depth was specified individually. The final design parameters were then used as input data for the scattering matrix program which produced the final theoretical radiation patterns. The detailed calculation of the scattering matrix for the device involved the cascading of 370 40-by-40 scattering matrices representing the straight sections and waveguide junctions making up the device.

The scattering matrix method calculates the matrix for each subsection of the total device (i.e., after 1 slot, 2 slots, . . . , up to 92 slots). From this we may determine the aperture modes that would be present if the device were terminated after any number of slots. The results of this calculation for a frequency of 34 GHz are shown in Fig. 2. The figure shows the increasing level of TM_{11} and decreasing level of TE_{11} as more slots are added, as well as a few of the other modes which are present. The final aperture modes and reflected modes are shown for the 92 slot device in Table 1. The aperture modes were then used to determine the E and H plane far field patterns of the feed. These results are shown in Figs. 3 and 4.

[1] See D. J. Hoppe, "Scattering Matrix Program for Circular Waveguide Junctions," Interoffice Memorandum No. 3335-84-071 (internal document), Dec. 5, 1984, Jet Propulsion Laboratory, Pasadena, CA.

The phase center of the feed was calculated as being exactly in the aperture plane. The efficiency of the 64-meter antenna in its present hyperboloid-paraboloid configuration, neglecting surface tolerance errors, was calculated using the theoretical patterns of Figs. 3 and 4. This efficiency was calculated to be 80.8% using the equivalent paraboloid method, and 79.5% using the GTD program (Ref. 8). Some theoretical results for the bandwidth were also determined. The calculated feed patterns for frequencies of 33.5 and 34.5 GHz are shown in Figs. 5 and 6, respectively. The theoretical antenna efficiency at 33.5 and 34.5 GHz was determined to be 81.0% and 80.4% respectively, both numbers being calculated using the equivalent paraboloid method.

A block diagram of the experimental test set up used on the mesa is shown in Fig. 7. The transition from single mode (0.368 I.D.) to multimode (1.75 I.D.) waveguide is a profiled circular waveguide taper. An ideal taper would produce a perfectly pure TE_{11} mode at the 1.75 I.D. end. For this particular taper the TM_{11} mode, which is the mode most strongly coupled to the TE_{11} mode in the taper, was measured to be about 29 dB below the TE_{11} mode at the taper output.

The measured patterns for the device are plotted in Figs. 3 and 4 for comparison. Excellent agreement is found in both planes with the best agreement in the H-plane. The slight differences in the E-plane may be accounted for by recalling that the calculated pattern is for a pure TE_{11} mode input, but in the experiment some spurious TM_{11} power is also present. The effects of this slight mode inpurity appear primarily in the E plane (see Ref. 8, Figs. 4 and 6). The experimental phase center of the feed was also determined to be in the aperture plane, which is also in agreement with theory.

IV. Conclusions

In conclusion, excellent agreement between the theoretical predictions of the scattering matrix program and experiment were obtained for a multimode corrugated feed section at 34 GHz. Since the program is also capable of analyzing corrugated horns of arbitrary profile and various other circular waveguide devices, it is expected to prove to be a valuable tool for analysis in the future.

Acknowledgments

The author would like to thank H. Reilly who supervised the fabrication of the various waveguide components and S. Stride who assisted in the pattern measurements.

References

1. Bhanji, A., Hoppe, D., Hartop, R., Stone, E., Imbriale, W., Stone, D., and Caplan, M., High power Ka-band transmitter for planetary radar and spacecraft uplink, *TDA Progress Report 42-78* (April-June 1984), Jet Propulsion Laboratory, Pasadena, CA, pp. 24–48.

2. Potter, P. D., and Ludwig, A., Antennas for space communications, *JPL Space Program Summary No. 37-26*, Vol. IV, Jet Propulsion Laboratory, Pasadena, CA, April 30, 1984, pp. 200–208.

3. Potter, P. D., A new horn antenna with suppressed sidelobes and equal beamwidths, *Microwave Journal*, June 1963, pp. 71–78.

4. Clarricoats, P. J., and Saha, P. K., Propagation and radiation behavior of corrugated feeds, Part 1, *Proc. IEE*, September 1971, pp. 1167–1176.

5. Dragone, C., Reflection, transmission and mode conversion in a corrugated feed, *Bell System Tech. J.*, July-August 1977, pp. 835–867.

6. Doane, J. L., Mode converters for generating the HE_{11} (Gaussian-like mode) from TE_{01} in circular waveguide, *Int. J. Elect.*, Vol. 53, December 1982, pp. 573–585.

7. James, G. L., Analysis and design of TE_{11} and HE_{11}, corrugated cylindrical waveguide mode converters, *IEEE Trans. Microwave Theory Tech.*, Vol. MTT-29, October 1981, pp. 1059–1066,

8. Hoppe, D., Imbriale, W., and Bhanji, A., The effects of mode impurity on Ka-band system performance, *TDA Progress Report 42-80* (October-December 1984), Jet Propulsion Laboratory, Pasadena, CA, pp. 12–23.

Table 1. Aperture and reflected modes for a pure TE_{11} mode incident on the feed

Modes	Percent of Incident TE_{11} Power, %	dB Below Incident TE_{11} Power, dBc
	Reflected Modes	
TE_{11}	0.0002	−58
TM_{11}	0.0012	−49
TE_{12}	0.0001	−62
TM_{12}	0.0010	−50
TE_{13}	< 0.0001	−65
TM_{13}	0.0015	−48
TE_{14}	< 0.0001	−65
TM_{14}	0.0054	−43
TE_{15}	0.0001	−62
	Aperture Modes	
TE_{11}	81.95	−0.86
TM_{11}	17.76	−7.5
TE_{12}	0.054	−33
TM_{12}	0.010	−40
TE_{13}	0.0013	−49
TM_{13}	0.2003	−27
TE_{14}	0.0003	−55
TM_{14}	0.0090	−40
TE_{15}	0.0008	−51

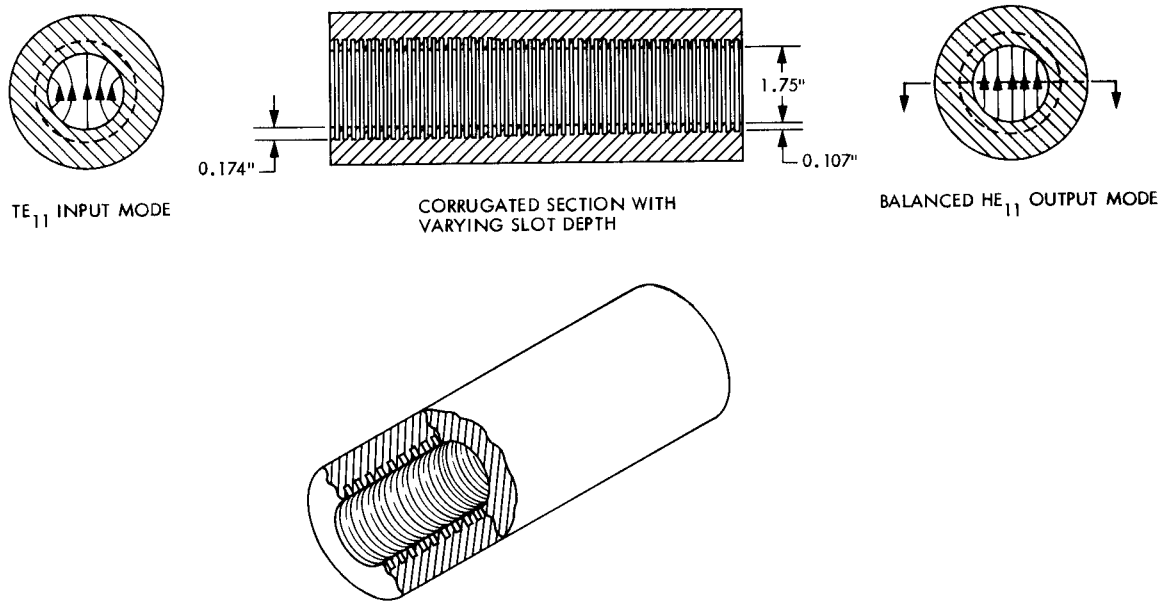

Fig. 1. The antenna feed

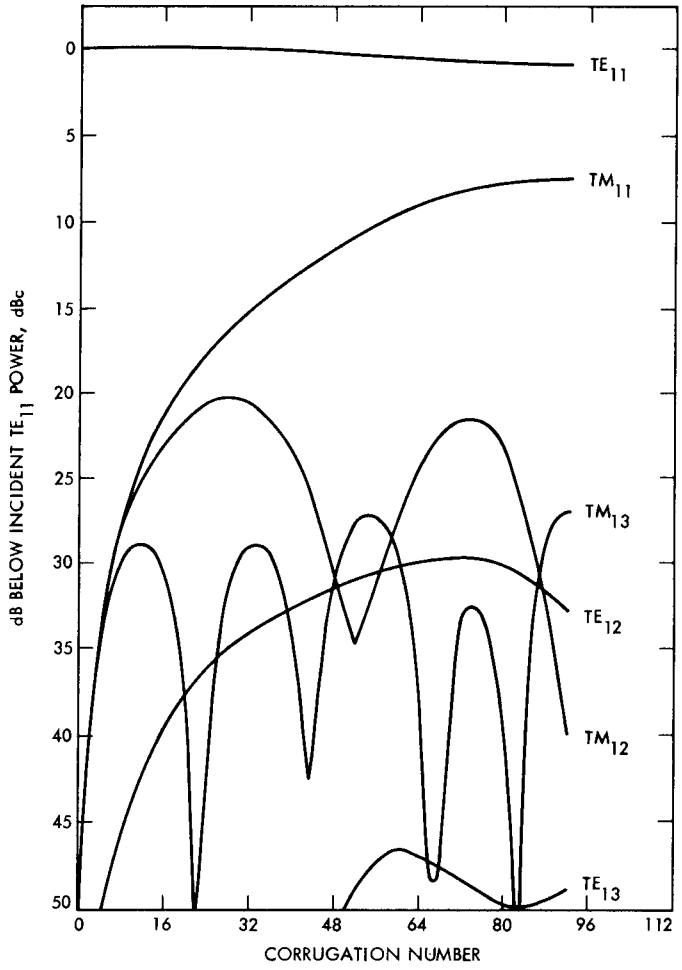

Fig. 2. Mode content vs corrugation number

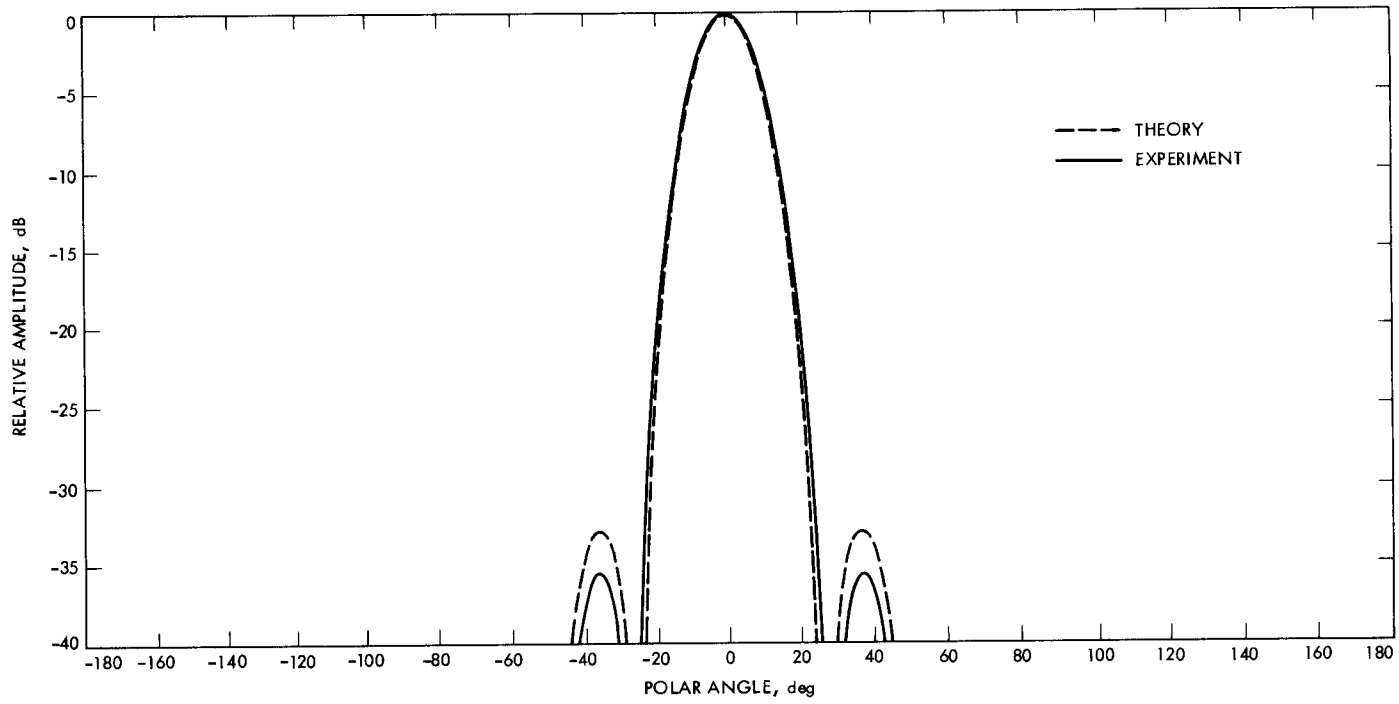

Fig. 3. Theoretical and experimental E-plane patterns at 34.0 GHz

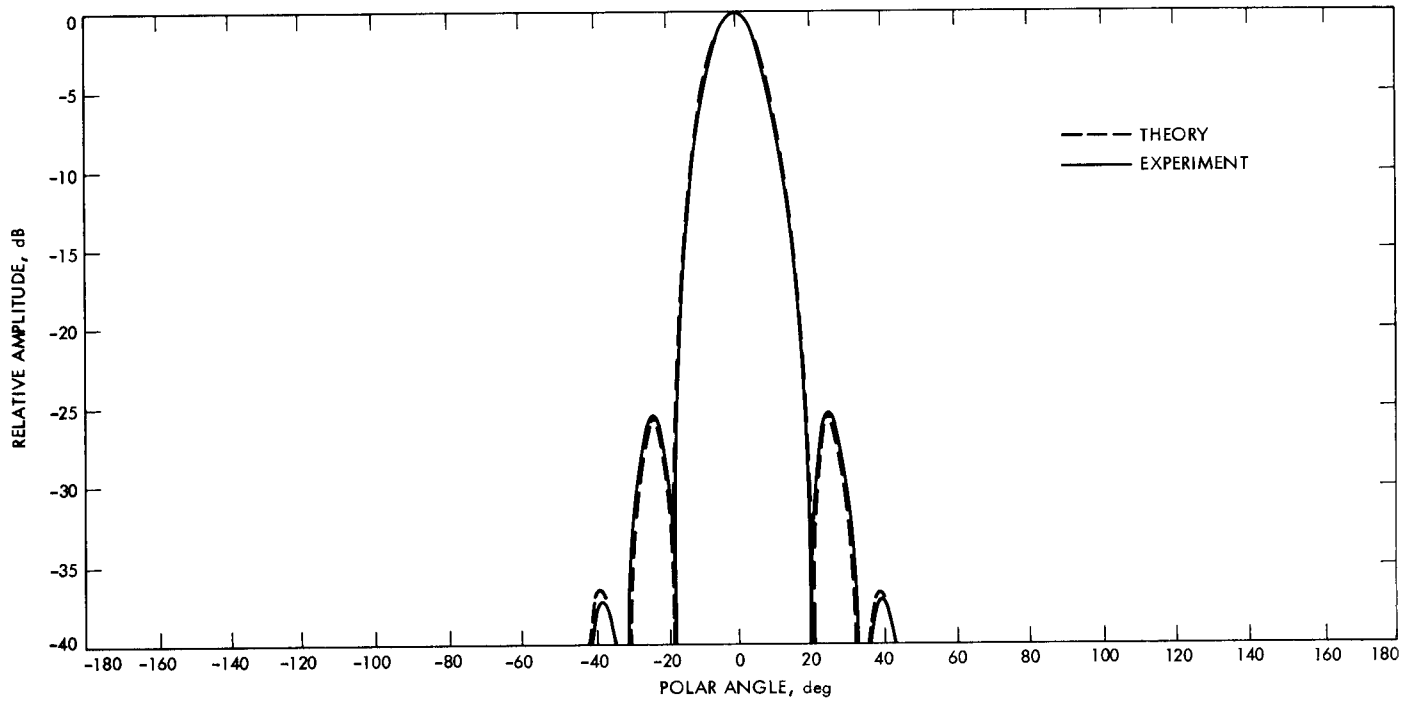

Fig. 4. Theoretical and experimental H-plane patterns at 34.0 GHz

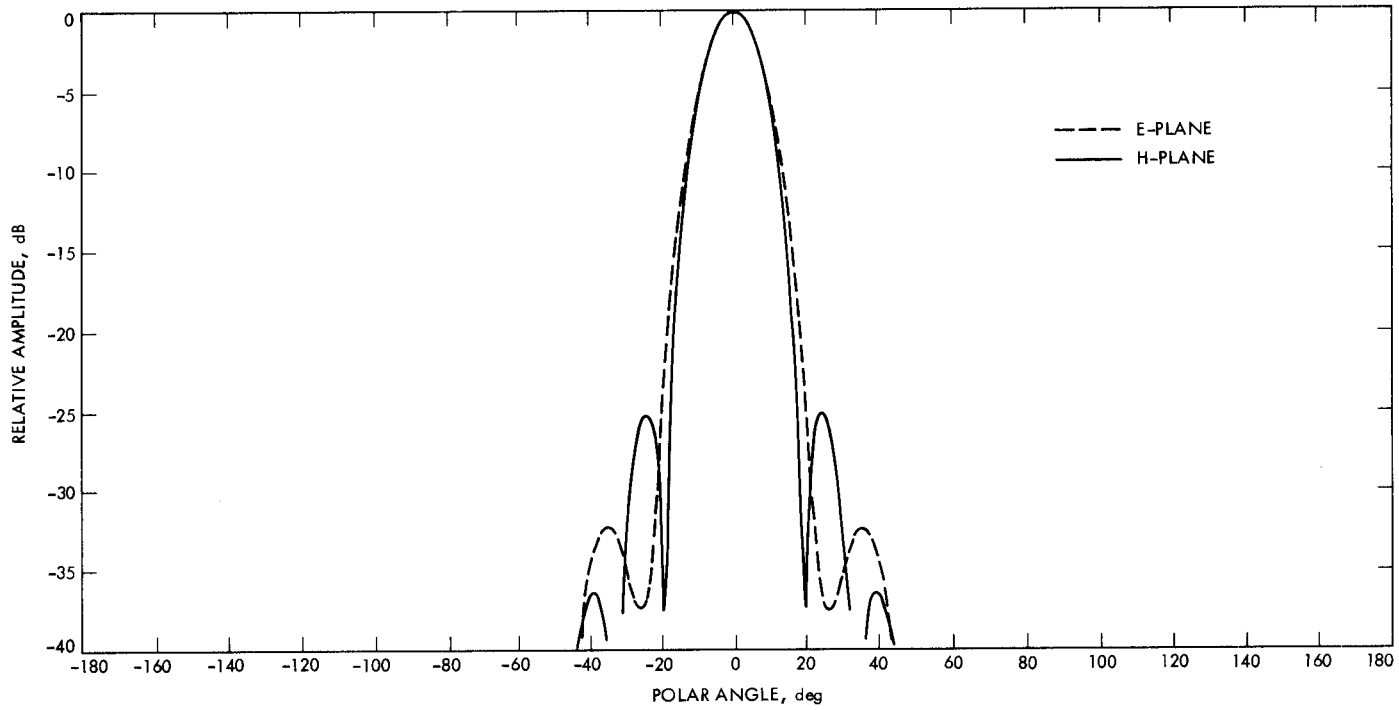

Fig. 5. Theoretical feed patterns at 33.5 GHz

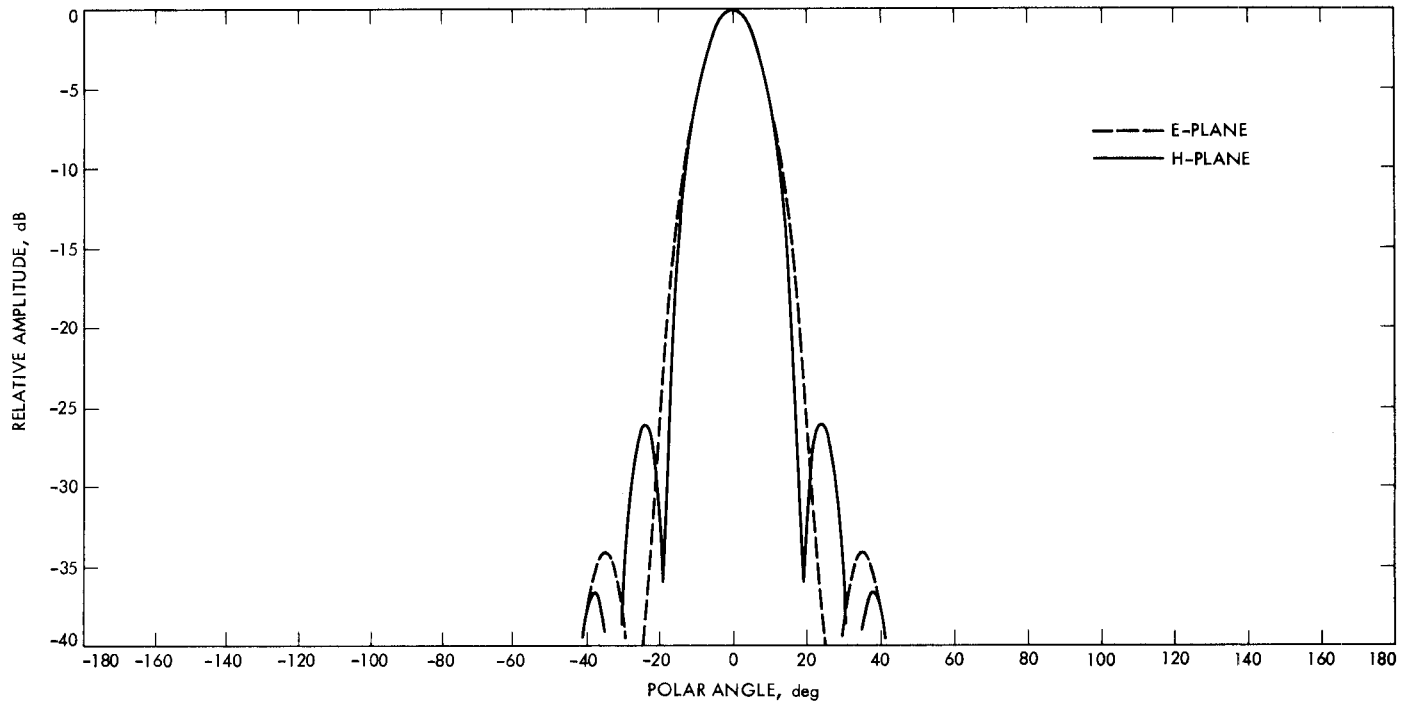

Fig. 6. Theoretical feed patterns at 34.5 GHz

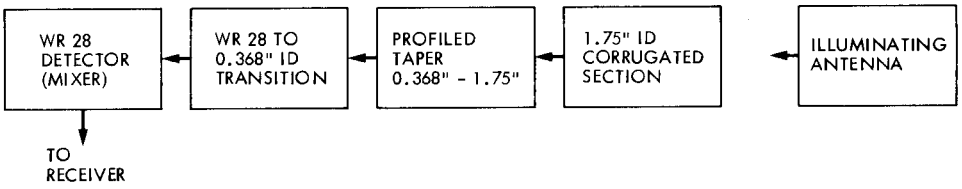

Fig. 7. Antenna range test set-up